MOLECULAR AND CELLULAR BIOLOGY, Jan. 1997, p. 416–426 Vol. 17, No. 1
0270-7306/97/$04.00+0

Active Mammalian Replication Origins Are Associated with a High-Density Cluster of ^{m}CpG Dinucleotides

THEO REIN,[1,2]* HARALABOS ZORBAS,[2] AND MELVIN L. DEPAMPHILIS[1]

National Institute of Child Health and Human Development, National Institutes of Health, Bethesda, Maryland 20892-2753,[1] and Department of Biochemistry, Ludwig Maximilians-Universität, D-81377 Munich, Germany[2]

Received 26 August 1996/Returned for modification 15 October 1996/Accepted 24 October 1996

ori-β is a well-characterized origin of bidirectional replication (OBR) located ~17 kb downstream of the dihydrofolate reductase gene in hamster cell chromosomes. The ~2-kb region of ori-β that exhibits greatest replication initiation activity also contains 12 potential methylation sites in the form of CpG dinucleotides. To ascertain whether DNA methylation might play a role at mammalian replication origins, the methylation status of these sites was examined with bisulfite to chemically distinguish cytosine (C) from 5-methylcytosine (^{m}C). All of the CpGs were methylated, and nine of them were located within 356 bp flanking the minimal OBR, creating a high-density cluster of ^{m}CpGs that was ~10 times greater than average for human DNA. However, the previously reported densely methylated island in which all cytosines were methylated regardless of their dinucleotide composition was not detected and appeared to be an experimental artifact. A second OBR, located at the 5′ end of the *RPS14* gene, exhibited a strikingly similar methylation pattern, and the organization of CpG dinucleotides at other mammalian origins revealed the potential for high-density CpG methylation. Moreover, analysis of bromodeoxyuridine-labeled nascent DNA confirmed that active replication origins were methylated. These results suggest that a high-density cluster of ^{m}CpG dinucleotides may play a role in either the establishment or the regulation of mammalian replication origins.

At least 16 initiation sites for DNA replication have now been mapped in the chromosomes of mammals (21, 32, 70). These studies have shown that DNA synthesis is not initiated randomly throughout cellular chromosomes but at specific DNA sites. However, these sites appear more complex than those found in the simpler genomes of bacteria, bacteriophages, yeasts, animal viruses, and mitochondria. Most DNA synthesis is initiated at specific genomic loci that are contained within 0.5 to 2 kb of DNA. These loci represent the functional origins of bidirectional replication (OBR). Replication bubbles also are detected throughout a larger initiation zone, ranging in size from 6 kb to greater than 55 kb, that encompasses the OBR and contains alternative initiation sites. Thus, metazoan cells appear to designate specific chromosomal loci as regions where initiation can occur and then to select from the many potential initiation sites within this region one site (or a small cluster of sites) that acts as a primary origin of DNA replication. What are the parameters that determine where DNA replication begins?

Metazoan replication origins are determined at least in part by specific DNA sequences. The same origins that are utilized in cells containing single copies of a unique genetic locus are also utilized in cells containing hundreds of copies of the same locus (12, 18, 39, 72). Moreover, origins can be translocated to other chromosomal sites and still retain their activity (33, 56) and origin activity can be eliminated by deletion of specific sequences (2, 41). Several reports of autonomously replicating sequence elements that function in mammalian cells and cell extracts have been documented in detail and shown to correspond to initiation sites for DNA replication in mammalian chromosomes (21). However, other studies have suggested that any sequence can act as an autonomously replicating sequence element (43). In addition, DNA replication can begin within virtually any DNA sequence under some conditions for transfecting cultured mammalian cells with plasmid DNA and when bare DNA is introduced into *Xenopus* eggs (30).

One explanation for these paradoxical results is that metazoan replication origins do not function properly outside the context of a cellular chromosome organized into a specific nuclear structure. Support for this explanation comes from the following experiments. Addition of either chromatin or bare DNA molecules to an extract from *Xenopus* eggs can result in the initiation of a single round of semiconservative DNA replication but only after the substrate has been assembled into nuclei containing nuclear lamins and functional nuclear pores (5, 16, 38, 54). However, replication under these conditions is initiated at many sites in the DNA that are apparently chosen at random. Site-specific initiation of DNA replication is observed only when the *Xenopus* extract is provided with intact nuclei isolated from differentiated cells (30, 31). In such cells, site specificity must be established in each cell division cycle during the middle of G_1 phase (76). The choice of initiation sites for DNA replication becomes more restricted during animal development (37), presumably as a consequence of changes in chromatin or nuclear structure and gene expression that accompany cell differentiation. Thus, nuclear structure is not only a prerequisite for site-specific initiation of DNA replication in metazoan chromosomes but may also directly select which of the many possible initiation sites in DNA will be used (see Jesuit Model in references 18 to 20).

One mechanism by which chromatin structure or nuclear organization might determine replication site specificity is DNA methylation. Methylated DNA can bind specific proteins (50, 53), change the hydrophilicity profile of the major groove, and influence DNA secondary structure (52). Recently, Tasheva and Roufa (68, 70) reported that an unusual densely methylated island (DMI) was associated with OBR in the chromosomes of proliferating, but not nonproliferating, mammalian cells. These DMIs consisted of from 127 to 516 bp, in

* Corresponding author. Mailing address: National Institute of Child Health and Human Development, Building 6, Room 416, National Institutes of Health, Bethesda, MD 20892-2753. Phone: (301) 402-1530. Fax: (301) 480-9354. E-mail: theorein@box-t.nih.gov.

TABLE 1. Primers that amplify unconverted DNA in CHO cell ori-β[a]

Primer	Position	Sequence
1	3475–3442	5′-ATA ATA AAA AAA CTA GTT TTG AGT CAT TTT ATG G
2	2128–2148	5′-TGA ACC AAT TCA AAT CTG ACC
3	2544–2521	5′-GTG TGG GAT TAT GCT ATA ACC CAC
4	2334–2354	5′-GCA CTT GCT CTG GAG ACC AGG
5	2353–2333	5′-CTG GTC TCC AGA GCA AGT GCC

[a] Primers 1D, 2D, 2E, 3D, 3E, 4C to 4E, 5D, 7D, and 8D are listed elsewhere (60).

which all cytosines on both strands were methylated, regardless of the dinucleotide composition. These observations strongly suggested that DNA methylation played a unique role in eukaryotic replication. However, application of three alternative methods employing hydrazine, permanganate, or methylation-sensitive restriction endonucleases for identification of methylated cytosines did not detect the DMI reported at ori-β downstream of the *DHFR* gene in Chinese hamster ovary (CHO) cells (60). Here we show that the bisulfite technique, when stringently applied, also fails to detect the proposed DMI at ori-β or ori-RPS14. These DMIs appear to be artifacts resulting from the inability of bisulfite to react with double-stranded DNA and from the use of PCR primers that selectively amplified the unreacted sequences. Nevertheless, mammalian replication origins contain numerous potential cytosine methylation sites in the form of CpG dinucleotides. In *Escherichia coli*, *oriC* contains numerous potential adenosine methylation sites in the form of GATC sequences and methylation at these sites plays an important role in regulating replication initiation (47). Since DNA methylation at CpG dinucleotides in mammalian cells affects both the timing of DNA replication and the activity of transcription promoters, we determined the methylation status of CpGs at replication origins.

Cytosines, but not methylcytosines, are converted to uracil in a reaction between bisulfite and single-stranded DNA, a change that is easily detected upon subsequent PCR amplification and sequence analysis. By this method, a high-density cluster of ^{m}CpG dinucleotides flanking the minimal OBR was identified at two mammalian replication origins in hamster cells. Moreover, analysis of nascent DNA strands confirmed that active replication origins were fully methylated. Since the methylation density in these regions was much greater than the average methylation density in mammalian DNA and the organization of CpG dinucleotides at other mammalian origins also carried the potential for similar methylation patterns, high-density clusters of ^{m}CpG dinucleotides may play a role in either the establishment or the regulation of mammalian replication origins.

MATERIALS AND METHODS

Bisulfite method. CHO K1 and CHOC 400 cells were grown and analyzed by fluorescence-activated cell sorter analysis as described elsewhere (60). Approximately 5×10^7 adherent cells were rinsed twice with phosphate-buffered saline on ice, scraped from the dishes with a rubber policeman, and collected by centrifugation at 1,000 × *g* for 5 min at 4°C. Cells were lysed in 5 ml of NIB buffer (30 mM Tris-HCl [pH 7.4], 10 mM NaCl, 1 mM $MgCl_2$, 5 mM $CaCl_2$, 0.5% Nonidet P-40) on ice for 10 min with gentle vortexing every 2 min. Nuclei were isolated by centrifugation through 2 ml of a 1 M sucrose cushion at 16,000 × *g* for 5 min at 4°C. The pellet was resuspended in 10 ml of NIB buffer containing 0.5% sodium dodecyl sulfate, incubated for 10 min at 50°C, and transferred to a 37°C bath. RNase A (100 μg/ml; Boehringer Mannheim) was added, and the incubation continued for 30 min. The sample was adjusted to 10 mM EDTA, proteinase K (100 μg/ml; Boehringer Mannheim) was added, and incubation continued overnight at 37°C. DNA was purified by organic extraction and ethanol precipitated. The pellet was resuspended in TE buffer (10 mM Tris-HCl [pH 7.8], 1 mM EDTA) to give a final concentration of ~200 μg of DNA/ml.

Several protocols for bisulfite conversion of cytosine to uracil in single-stranded DNA have been described in the literature (15, 25, 68). The most complete conversion (as checked by analysis with nonselective primers) was obtained by the following protocol. It was essential to cut the DNA in small pieces (i.e., as small as possible to still allow primer annealing) to obtain efficient bisulfite conversion. Purified DNA was digested with the restriction endonucleases *Apa*I, *Bam*HI, *Bcl*I, *Hin*dIII, *Nhe*I, *Eco*RI, *Pst*I, *Eco*RV, and *Xho*I. Each digestion was carried out for 2 h at 37°C in the buffer recommended by the manufacturer (Boehringer Mannheim). Several enzymes were included in a single digestion when possible. The DNA products were then extracted with phenol, precipitated with ethanol, and redissolved in 50 μl of TE buffer. The digested DNA had an average length of ~1 kb, as visualized after gel electrophoresis and ethidium bromide staining.

DNA was denatured by adjusting a 5-μl sample containing 2 μg of genomic DNA or a PCR fragment (control) to 0.3 M NaOH (freshly prepared) in a final volume of 20 μl and then incubating the mixture for 15 min at 37°C. Cytosines were sulfonated by adding 120 μl of 3.6 M sodium bisulfite (reagent grade, freshly prepared, and adjusted to pH 5.0 with 10 M NaOH; Sigma) in 0.6 mM hydroquinone (freshly prepared) and incubating the sample in a Perkin-Elmer model 9600 thermocycler (the sample was split into two tubes to fit in the thermocycler) for a period of 5 h by the following cycling protocol: 30 s at 95°C and then 15 min at 50°C. The DNA sample was then desalted by using the Wizard purification system (Promega) and desulfonated as described previously (15).

DNA sequences were amplified by mixing 20 ng of bisulfite-treated DNA with 100 pmol of each PCR primer in 50 μl of reaction buffer containing 200 μM concentrations of each of the four deoxynucleoside triphosphates. *Taq* polymerase (2 U; Boehringer Mannheim) was added, and the sample was incubated in a Perkin-Elmer model 9600 thermocycler for 1 min at 95°C, 1 min at 50°C, and 1 min at 72°C for a total of 30 cycles. The PCR products were separated by electrophoresis through a low-melting-point agarose gel. The product of interest was cut from the gel, purified by isotachophoresis (55) or with a gel extraction kit (Promega or Qiagen), and sequenced with an internal primer and a cycle sequencing kit (Amersham). In some cases, selectivity was improved either by subjecting the PCR amplification product to a second PCR amplification with internal primers or by increasing the annealing temperature, in increments of 2°C, to 64°C in an effort to select for rare molecules.

The most reliable sequence available for ori-β is a compilation of several independent analyses of the genomic sequence in this region of the CHO cell genome (GenBank accession number X94372). The nucleotide positions given throughout this communication refer to this sequence.

Artificial DMI boundary. An artificial DMI boundary containing ori-β sequences was created by joining together two synthetic fragments, one methylated and one unmethylated. Oligonucleotides BclI (5′-TAC TGA TCA GGT GTG GCC TTG TTG GAA GAA GTG) and 1D (Table 1) were used to synthesize an ~650-bp PCR fragment from pneoS13 (3) in the presence of 5-methyl-dCTP. The restriction site is underlined. Oligonucleotides BamHI (5′-ATG GGA TCC ACT CAC TCT GAG CCT ATG GGG CCA) and 4D (Table 1) were used to synthesize an ~200-bp-long PCR fragment in the presence of dCTP. The products were cut with *Bam*HI or *Bcl*I and ligated. The artificial DMI boundary fragment (~850 bp) was purified by agarose gel electrophoresis.

Analysis of nascent DNA. CHO K1 cells were seeded into 150-mm-diameter tissue culture dishes and cultured at 37°C in 5% CO_2 in Dulbecco modified Eagle medium supplemented with 10% fetal bovine serum and nonessential amino acids. When cells reached 20% confluence, 1 μg of aphidicolin (Bethesda Research Laboratories) per ml was added for 24 h to synchronize them at the boundary of G_1 and S. Cells were washed twice with prewarmed medium to remove the aphidicolin, cultured for 12 h in the absence of drug, and then cultured for an additional 12 h in the presence of drug. Cells were released from their final aphidicolin block and cultured for 14 min before nascent DNA was pulse-labeled for 1 min by addition of 100 μM bromodeoxyuridine (BrdU). Cells were then washed twice with prewarmed medium and cultured in fresh prewarmed medium for 6 h. Cells were washed twice with 20 ml of ice-cold phosphate-buffered saline containing 0.02% Na-azide before 5 ml of 10 mM Tris-HCl–1 mM EDTA–100 mM NaCl was added and the cells were scraped off the dish with a rubber policeman. Once cells were exposed to BrdU, all steps were carried out in the absence of direct sunlight or room lights. DNA was isolated and cut with restriction endonucleases as described above. Br-labeled DNA was then isolated by affinity chromatography with an anti-BrdU antibody column (71).

TABLE 2. Primers that amplify converted DNA in CHO cell ori-β

Primer	Position	Sequence[a]
Antisense strand		
1a	3475–3442	5′-ATA ATA AAA AAA TTA GTT TTG AGT TAT TTT ATG G
2a	2128–2148	5′-TAA ACC AAT TCA AAT CTA ACC-3′
3a	3544–3521	5′-GTG TGG GAT TAT GTT ATA ATT TAT
4a	2334–2354	5′-ACA CTT ACT CTA AAA ACC AAA
5a	2353–2333	5′-TTG GTT TTT AGA GTA AGT GTT
6a	2675–2703	5′-TTC TCA ATA AAT CCA CTT ACT TTA AAA TC
7a	2898–2870	5′-TGT GTT TTT TGA AAA ATT TGT TTT TAT GT
8a	3421–3395	5′-AGT TTT ATT AGA AAT AGT AAG TTG GGG
9a	3049–3023	5′-GTT TAG AGT TTA TTT AAT TGA TGT TAT
10a	1598–1617	5′-TAT ATA ACT CCT TCC CAA CC
11a	1681–1701	5′-AAA ATA CAA ATA AAC CAT ACC
12a	1928–1909	5′-TTA GTA TAT TAA TTT AAA TG
13a	1944–1925	5′-GGA TAA TGT ATT TTA TTT AG
14a	1702–1682	5′-TGG TAT GGT TTA TTT GTA TTT
15a	1577–1598	5′-ATA AAC ACA AAA AAA TCC ATT A
16a	2313–2334	5′-ATA ACT TTA AAA CCT ATC CTA A
17a	2500–2479	5′-TTG ATT ATT TGA TAT TAG TTG G
18a	3440–3413	5′-TTT TTA AGA TTA TTT ATT AAG TTT TAT T
19a	3023–3049	5′-ATA ACA TCA ATT AAA TAA ACT CTA AAC
20a	3408–3384	5′-ATA GTA AGT TGG GGT ATA AGT TAT T
21a	3394–3372	5′-TAT AAG TTA TTT TGT AGT TTT GG
22a	2807–2785	5′-GGT TGA ATT TTA TTA GTG TAG TG
23a	2220–2199	5′-GAT GTG ATG GTA TTT TAT GAT T
24a	1501–1522	5′-AAA AAT TTC TAT AAC CTC CAA A
25a	1617–1596	5′-GTT GGG AAG GAG TTA TAT AAT G
26a	3758–3737	5′-AAG AGG GTA TTG GAG TTT TTA G
27a	3584–3605	5′-TTC TCT ATA TAA CTT TAA AAC C
28a	3713–3693	5′-GTT AGG TGT TGG TGG TGT ATG
Sense strand		
1s	3475–3442	5′-ATA ATA AAA AAA CTA ATT TTA AAT CAT TTT ATA A
2s	2128–2148	5′-TGA ATT AAT TTA AAT TTG ATT
3s	2544–2521	5′-ATA TAA AAT TAT ACT ATA ACC CAC
4s	2334–2354	5′-GTA TTT GTT TTG GAG ATT AGG
5s	2353–2333	5′-CTA ATC TCC AAA ACA AAT ACC
6s	2675–2703	5′-TTT TTA GTG AGT TTA TTT GTT TTA AAA TT
7s	2898–2870	5′-TAT ATT TTC TAA AAA ACC TAC CTT CAT AC
8s	3421–3395	5′-AAT CTC ATC AAA AAT AAC AAA CTA AAA
9s	3049–3023	5′-ATT CAA AAT CTA CCT AAC TAA TAT CAC
10s	1598–1617	5′-TGT GTG GTT TTT TTT TAG TT
11s	1681–1701	5′-AGG ATG TAG ATA AGT TAT GTT
12s	1928–1909	5′-CCA ACA TAC TAA TAT AAA TA
13s	1944–1925	5′-AAA CAA TAT ATT TTA CCC AA
14s	1702–1682	5′-TAA CAT AAC TTA TCT ACA TCC
15s	1577–1598	5′-ATA GAT ATA AAG GAA TTT ATT G
16s	2313–2334	5′-GTA GTT TTG GAG TTT ATT TTG G
17s	2500–2479	5′-CTA ACT ATC TAA CAC CAA CAC CAA CTA A
23s	2219–2199	5′-ATA TAA TAA CAT TTT ATA TCC
24s	1501–1522	5′-AGG AGT TTT TAT GGT TTT TAA G
25s	1623–1602	5′-AAC TTA ACT AAA AAA AAA CCA C
26s	3762–3741	5′-CCA AAA AAA AAC ATT AAA ACT C
27s	3592–3571	5′-TTT AAG ATA GGG TTT TTT TGT G
28s	3711–3691	5′-CAA ATA TTA ATA ATA CAT ACC
Nonselective primers		
C1	2740–2762	5′-TAA TAA TAA ATA TCT TCT CTT AC
C2	2935–2915	5′-TTA ATG ATT ATG GAT TAG AGG

[a] Mutated bases are underlined.

RESULTS

Identification of ^{m}CpGs at two replication origins, ori-β and ori-RPS14. ori-β contains an OBR that has been mapped by a variety of methods to a position ~17 kb downstream of the *DHFR* gene in Chinese hamster ovary cells (reviewed in references 18 to 20 and 30). This OBR is located within a 55-kb initiation zone. By the technique of competitive PCR (29), the hypothesis that most initiation events occur at the OBR site within this initiation zone has been tested recently by quantifying the relative abundance of nascent DNA strands. Initiation events at ori-β were found to be localized within an ~2-kb segment where the frequency of initiation events was 10 to 20 times greater than in flanking sequences distributed throughout the 110-kb region encompassing ori-β (42, 57). Therefore, the methylation state of this ~2-kb region was examined in detail.

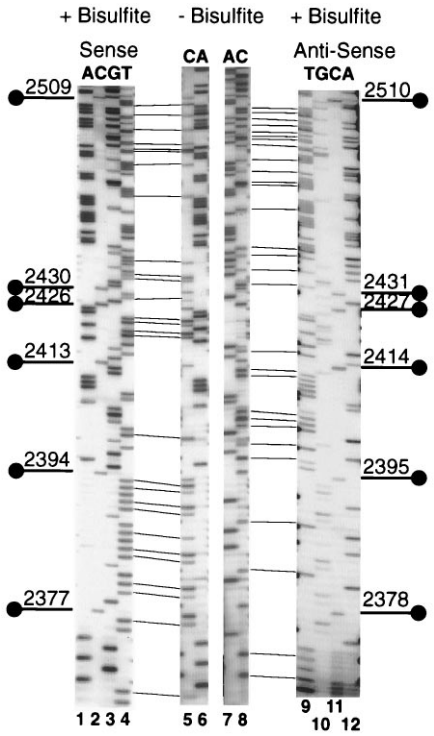

FIG. 1. Methylation sites within ori-β, positions 2368 to 2516. In lanes marked − Bisulfite, PCR primers 2 and 3 (Table 1) were used to amplify ori-β nucleotides 2128 to 2544 from a CHO K1 genomic DNA template. The PCR products were sequenced with primer 4 (Table 1). In lanes marked + Bisulfite, total DNA was purified from proliferating CHO cells and reacted with bisulfite. Sense-strand DNA (with reference to transcription of the *DHFR* gene) was selectively amplified with primers 2s and 3s and sequenced (lanes 1 to 4) with primer 4s. Antisense-strand DNA was selectively amplified with primers 2a and 3a and sequenced (lanes 9 to 12) with primer 4a. Primer sequences are given in Table 2. Thin lines connect those cytosines in the DNAs in lanes labeled − Bisulfite that were converted to thymines in the DNAs in lanes labeled + Bisulfite. The positions of cytosines that were not converted by bisulfite are identified by lollipops. Reference sequences are in lane 5 (for lanes 2 and 10), lane 6 (for lanes 1 and 9), lane 7 (for lanes 4 and 12), and lane 8 (for lanes 3 and 11).

Methylated cytosines in the genomic DNA of mammalian cells can be detected at high sensitivity by converting cytosines in single-stranded DNA to uracils in the presence of bisulfite and then using PCR to amplify the sequences of interest (27). Primers (Table 2) were designed to selectively amplify the converted sense or antisense strand of bisulfite-reacted DNA. In order to anneal to converted DNA, the first primer usually contained four to five adenosines in place of guanosines (e.g., primer 4a) (Table 2). The second primer, designed to anneal to the extension product of the first primer, contained thymines in place of cytosines (e.g., primer 3a) (Table 2). To reveal the methylation state of the total cell population, PCR products were purified by agarose gel electrophoresis and then sequenced directly. This strategy avoided possible selection artifacts introduced by cloning the PCR DNA products and sequencing individual molecules (15). Both genomic strands were analyzed.

The results of this analysis revealed that all of the CpG dinucleotides within the ~2-kb region encompassing ori-β were methylated. For example, methylation sites within positions 2368 to 2516 are shown in Fig. 1. The sense strand of this sequence contained 34 cytosines, 28 of which were converted by bisulfite treatment into uracil and then by PCR amplification into thymines (compare the reference DNA sequence in lane 5 to the sense-strand sequence of bisulfite-reacted DNA in lane 4). Six of the cytosines were not converted by bisulfite treatment, and therefore these cytosines were methylated (compare the remaining cytosines in lane 5 with the cytosines that appear in lane 2). Each of these methylated cytosines was part of a CpG dinucleotide. Further analysis of the antisense strand revealed that of the 35 cytosines present, the same six CpG dinucleotides were methylated, as expected. Analysis of all CpG dinucleotides from map positions 1500 to 3700 revealed the presence of 16 methylated CpG dinucleotides (Fig. 2). This represented all of the CpGs within this sequence. None of the other cytosines were methylated. The same 16 ^{m}CpGs were observed in both proliferating and serum-arrested CHO cells, as well as in proliferating CHOC 400 cells containing ~1,000 copies of the *DHFR* gene region (data not shown).

To determine whether the methylation pattern observed for ori-β was typical of replication origins in CHO cells, the same experiments were carried out at a second OBR, at ori-RPS14, located within a 2-kb region at the 3′ end of the gene encoding ribosomal protein S14 (69). The results revealed that each of the 19 CpG dinucleotides in this region contained methylated cytosine on both strands, although four of them were methylated in about 20 to 60% of the DNA analyzed (see Fig. 7 for a summary). For example, all the cytosines in the region containing the putative DMI (see below) were converted to uracils and then to thymines, except for a cluster of five cytosines within the indicated CpG dinucleotides (Fig. 3, compare lane 3 with lane 7 and lanes 1 and 3 with lane 5). Therefore, these five cytosines must be methylated. The intensities of the T bands relative to the intensities of their corresponding C bands indicated that at least 95% of the DNA contained the indicated methylation pattern.

Searching for the DMI in ori-β and ori-RPS14. Using the bisulfite method for detecting ^{m}C, Tasheva and Roufa (68) reported the existence of an unusual DMI flanking the OBR mapped at ori-β and at ori-RPS14 (Fig. 2; also see Fig. 7). The DMI at ori-β encompassed 516 bp, and the DMI at ori-RPS14 encompassed 127 bp. These DMIs were reported to exist in ~90% of proliferating CHO cells but to be absent in serum-arrested cells; however, they were not detected in the experiments described above.

Experimentally, a DMI is recognized as a sequence in which all of the cytosines on both strands are methylated and in which a clear transition between methylated and nonmethylated sequences can be demonstrated. Therefore, to detect a DMI by the bisulfite method, any one of the following three primer sets can be used in the PCR step to amplify the DMI region. The first primer set contains one primer that anneals to converted sequences (contains U instead of C) outside the DMI and one primer that anneals to unconverted sequences (contains C) within the DMI. This primer set selects for the transition from converted to unconverted DNA that marks one of the boundaries of a DMI. The second primer set anneals to converted sequences that lie on both sides outside the DMI. These primers select for a complete DMI in which both boundaries are represented. Selection of specific sequences is expected to be determined solely by the primers used and not by the intervening sequences that are amplified by the primers. The third primer set is nonselective. One primer anneals to sequences devoid of cytosines, while the second primer anneals to sequences devoid of guanosines. This primer set gives an unbiased representation of the fraction of molecules that contains converted or unconverted DNA. All three strategies were applied to ori-β and ori-RPS14, but in no case was a DMI de-

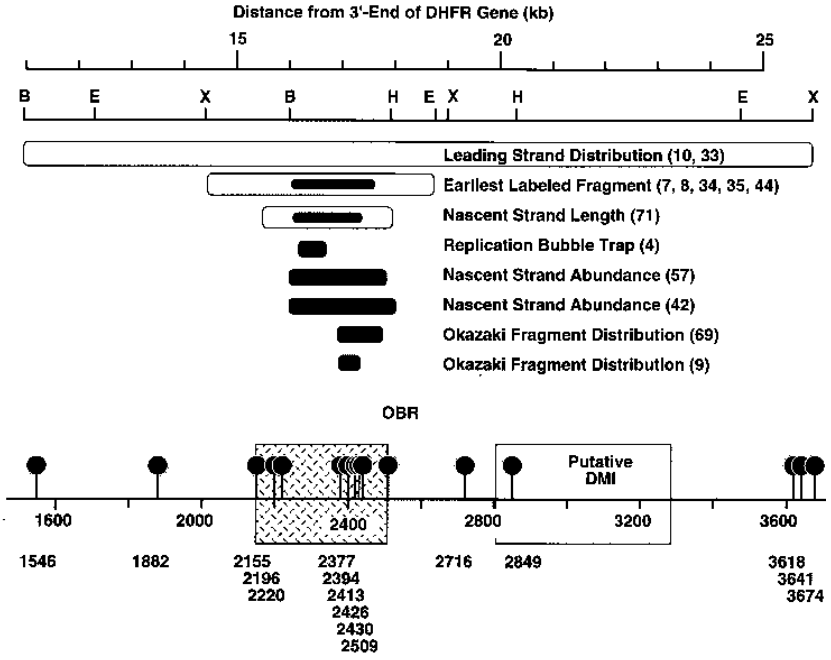

FIG. 2. Methylated DNA at ori-β. Most initiation events that occur within a 120-kb region of the CHO cell genome located in and around the *DHFR* gene occur within an ~2-kb locus (the shaded area was determined by nascent-strand abundance assays [42, 57]) located ~17 kb downstream of the *DHFR* gene, referred to as ori-β. This conclusion is based on the results contained in 13 publications from seven different laboratories by six different strategies for mapping the origins of nascent DNA strands. The OBR lies within the region from positions 2435 to 2918, where a transition from discontinuous to continuous DNA synthesis occurs on each template strand, as determined by mapping the distribution of Okazaki fragments (9). The map locations (GenBank accession number X94372) of the 16 ^{m}CpGs identified within this region are given. The stippled box indicates a 356-bp region containing nine ^{m}CpGs. The open box indicates the position of the putative DMI reported by Tasheva and Roufa (68). The black lollipop symbol indicates an ^{m}CpG. Restriction endonuclease sites are indicated as B (*Bam*HI), E (*Eco*RI), X (*Xba*I), and H (*Hin*dIII).

tected. An example of the nonselective primer strategy as applied to ori-RPS14 is shown in Fig. 3.

We considered the possibility that the discrepancy between the results of Tasheva and Roufa (68) and those reported here was due to primer design. For example, both members of the primer set (P11 and P12) used by Tasheva and Roufa (68) to amplify the ori-β DMI annealed to unconverted sequences outside the putative DMI. This is opposite to the strategy that one would have anticipated, as explained in the rationale noted above. When we applied this primer strategy to the ori-β DMI, all of the cytosines in the amplified DNA were unconverted (Fig. 4, lanes 5 to 8). Conversely, when both primers annealed to converted DNA, all of the cytosines in the amplified DNA were converted, except for the single ^{m}CpG at position 2850 (Fig. 4, lanes 1 to 4). These results are consistent with what one would have expected from the theory, if one considers that a fraction of the template DNA is resistant to bisulfite conversion. It is known that bisulfite does not react with double-stranded DNA (27). Therefore, the unconverted cytosines in non-CpG dinucleotides observed in our experiments likely reflect the extent to which these DNA samples were denatured in the presence of bisulfite. In fact, it was possible to obtain amplified DNA containing fully unconverted cytosines even with PCR-generated template DNA that did not contain ^{m}C. In our hands, the fractions of unconverted DNA were found to vary greatly as a function of DNA fragment length, temperature of the bisulfite incubation, and PCR cycling parameters. Quantitation of the efficiency of cytosine conversion by bisulfite with nonselective primers revealed that our protocol yields greater than 95% conversion of the genomic DNA.

The above-noted observations suggest that the most reliable results are those where unconverted cytosines are present in amplified DNA that also contains converted cytosines, such as would occur at an ^{m}CpG or at a DMI border. To determine whether a DMI would have been detected if it existed, an artificial ori-β DMI, containing a transition between methylated and unmethylated cytosines, was constructed and subjected to the bisulfite method. A clear transition from unconverted to converted DNA was observed at the artificial DMI boundary: all cytosines within the DMI were present (Fig. 5, lane 3), while all cytosines outside the DMI were replaced by thymines (Fig. 5, compare lane 3 with lane 1). This transition was detected even when genomic DNA was present in 100-fold molar excess of the quantity of artificial DMI, demonstrating that the proposed DMI could have been detected in our experiments if it was present in as little as 1% of the genomic DNA.

Finally, we considered the possibility that our DNA did not exhibit a DMI because of differences in cells, culture conditions, or DNA preparations. To address this problem, Tasheva and Roufa graciously provided two DNA samples. One sample was high-molecular-weight genomic DNA from proliferating CHO K1 cells, and the other sample contained the same DNA treated with bisulfite. In our hands, these two DNA samples gave results identical to those with our own DNA preparations. All CpG dinucleotides were methylated, but the putative DMI was absent. However, using nonselective primers, we determined that less than 5% of Tasheva and Roufa's DNA had been converted in their bisulfite-treated sample in contrast to the more than 95% conversion efficiency obtained with the samples reacted in our lab. Taken together, the results described above strongly suggest that the DMIs reported at ori-β

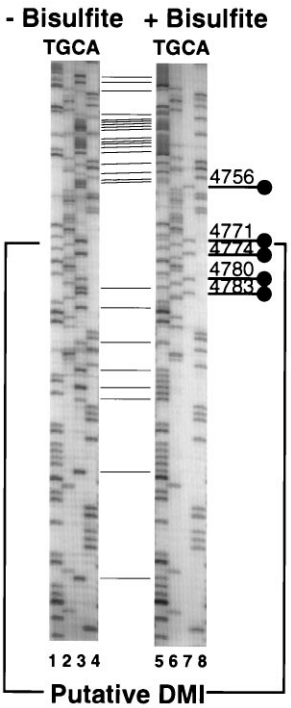

FIG. 3. Methylation sites within ori-RPS14, positions 4835 to 4706 (GenBank accession number M35008). The portion of the sequence that contains the putative DMI is bracketed. In lanes labeled − Bisulfite, PCR primers C3 and C6 (Table 3) were used to amplify nucleotides 4632 to 5036 of CHO K1 cell genomic DNA within ori-RPS14. The PCR products were sequenced with primer C4 (Table 3). In lanes labeled + Bisulfite, the same primers were applied to bisulfite-reacted DNA. Thin lines connect those cytosines in the reference DNA (lanes labeled − Bisulfite) that were converted to thymines in bisulfite-treated DNA (lanes labeled + Bisulfite). Cytosines that were not converted by bisulfite are identified by lollipops. Lanes 1 to 4 provide the reference sequences for lanes 5 to 8, respectively.

and ori-RPS14 did not result from DNA methylation but rather from incomplete bisulfite reaction and selective primer design (see Discussion).

The same pattern of high-density ^{m}CpGs was also found at active origins. Both ori-β and ori-RPS14 are early-firing replication origins. The presence of a high-density cluster of ^{m}CpG dinucleotides at such origins was surprising, because methylated DNA is usually associated with late-replicating DNA and with transcriptionally inactive chromatin. Moreover, it has been suggested that DNA methylation inactivates replication origins in *Physarum* ribosomal DNA (15a). Therefore, we considered the possibility that while the bulk of origin sequences were methylated, only a small, unmethylated fraction of the total ori-β sequences was actually active, and this fraction was not detected by analysis of total chromosomal DNA. To test this hypothesis, the methylation status of nascent DNA that originated from ori-β was analyzed. Mammalian methyltransferase methylates predominantly, if not exclusively, at hemimethylated CpG sites (14). Therefore, if active parental ori-β DNA is methylated, nascent DNA originating from these sequences will become methylated while nascent DNA from unmethylated origins will be unmethylated.

CHO cells synchronized at the G_1-S border were released into S phase, and newly synthesized DNA was pulse-labeled with BrdU. DNA was isolated 6 h after the pulse and digested with restriction endonucleases. Nascent DNA was isolated by affinity chromatography and analyzed for ^{m}C by the bisulfite method. The ori-β fragment was cut away from flanking sequences to ensure that all ori-β sequences subsequently isolated by their affinity for anti-BrdU antibodies actually contained BrdU and were not simply linked to sequences that were labeled some distance away due to initiation at nearby upstream or downstream origins. The same pattern of methylation described for ori-β in total DNA was observed for ori-β in nascent DNA (Fig. 6). Thus, active replication origins were, in fact, fully methylated.

DISCUSSION

Methylation of CpG dinucleotides at mammalian replication origins. Stringent application of the bisulfite method to distinguish cytosine (C) from 5-methylcytosine (^{m}C) revealed that at least 2 of the 16 mammalian replication origins that have been mapped to specific genomic locations (21, 32, 70) are methylated at each of the CpG dinucleotides located in and around their OBR. Sixteen ^{m}CpGs were found within the ~2-kb region that exhibits greatest replication initiation activity at ori-β (Fig. 2). Nine of these are clustered within a 356-bp region (2155 to 2510) to one side of the functional OBR. Eight of these ^{m}CpGs are clustered within 273 bp (2155 to 2427), and five reside within 51 bp (2377 to 2427). Since the average density of ^{m}CpG dinucleotides in the human genome is approximately one per 330 bp (74), the density of ^{m}CpGs in ori-β is 8- to 33-fold greater than average. This pattern of hypermethylated CpGs appeared at all ori-β loci, both in single-copy CHO cells and in the highly amplified tandem repeats of the *DHFR* gene region present in CHOC 400 cells. Of greatest importance, this pattern of methylation was present at active as well as inactive copies of ori-β.

ori-β was not unique in this respect. All of the 19 CpGs in ori-RPS14 were methylated, although four of them were methylated in about 20 to 60% of the DNA analyzed (Fig. 7). Nine were clustered within a 354-bp region (3579 to 3932) to one side of the OBR, and five were clustered within a 171-bp region within the OBR. Thus, both ori-β and ori-RPS14 contain at least one cluster of ^{m}CpG dinucleotides with at least one ^{m}C per 40 bp flanking their OBR.

The pattern of CpG dinucleotides at other mammalian replication origins suggests three methylation motifs. The first motif is exemplified by ori-β and ori-RPS14. A high-density cluster of ^{m}CpG dinucleotides containing at least one ^{m}C per 40 bp flanks the OBR. This group may include the late-S-phase origin mapped about 150 kb from the 3′ end of the *ADA* gene (72), which contains a cluster of 10 CpGs within 356 bp, and the origin at the 5′ end of the rhodopsin gene (28), which contains a cluster of 23 CpGs within 498 bp. Whether these sites are methylated in vivo remains to be determined. The second motif is represented by replication origins that lie within sequences so rich in CpG dinucleotides that they can potentially be methylated at a density of one ^{m}C per 12 to 20 bp over regions 1 to 7 kb in length. This group includes replication origins located within the CpG-rich promoters of genes like the human lamin B2 gene (29), mouse, rat, and human ribosomal genes (32, 78), and the c-*myc* gene (4, 49). In general, regulatory sequences rich in CpG dinucleotides (CpG islands) are not methylated in transcriptionally active genes (13, 24, 26, 58). However, the extent of methylation in the CpG island at the mouse ribosomal gene promoter, for example, depends on the cell line (59) as well as on the age of the cells (66). Therefore, it is possible that some or all of the CpGs in these CpG islands are methylated when they are associated with active replication origins. The third methylation motif contains CpG dinucleotides, but their pattern does not allow

TABLE 3. Analyses of the CHO cell ori-RPS14

Primer	Position	Sequence[a]
Primers that amplify unconverted DNA		
1	4699–4726	5′-GCA ATG ACA TTT TTT CTT CTT GCA GAG G
2	4992–4969	5′-CCT AAG GTC ACC GGG GTG TGG TGG
11	4832–4850	5′-GTA TAA GCT ATT TTG GTT C
12	4850–4832	5′-GAA CCA AAA TAG CTT ATA C
Primers that amplify the antisense strand		
1a	4699–4726	5′-ACA ATA ACA TTT TTT CTT CTT ACA AAA A
2a	4992–4969	5′-TTT AAG GTT ATT GGG GTG TGG TGG
3a	4653–4675	5′-ACT AAT TAA TCT AAT AAC TAA AA
4a	4676–4699	5′-AAA CTA TAT TTA TAT AAC TAT AAA
5a	4705–4726	5′-ACA TTT TTT CTT CTT ACA AAA A
6a	4973–4952	5′-GGT GGT GTA TTT TTT TAT TTT T
7a	5010–4991	5′-GTG TTG TTT TGG GTG GTT TT
8a	5051–5027	5′-TTT TAT ATG TAA TTT TAA TAT TTT T
11a	3534–3553	5′-TAA ACA TAA TAA CTC ACA CC
12a	3693–3673	5′-TTA GTT TTA AGA GAT TTA TGG
13a	3670–3690	5′-AAA CCA TAA ATC TCT TAA AAC
14a	3987–3968	5′-AAG ATT TGT ATA TTG TGA GG
15a	3470–3489	5′-CAC AAA CCA AAT AAC TAT CC
16a	3672–3651	5′-TTT TTT TTT GTT TTT TAT AGG G
17a	3698–3718	5′-ACT AAA CCA CCT CTC CAA ACC
18a	3960–3939	5′-ATA AAA TTT TAG ATT TTG TAG G
19a	3959–3980	5′-ATA TAA TCC CCT CAC AAT ATA C
20a	4087–4107	5′-AAA CCT AAA ACC CAA TCA ACC
21a	4184–4164	5′-AAT AAA TTT AAT GTT AGT TAG
22a	4458–4479	5′-AAA CAA ACA ACC ACA AAT ACT C
23a	4627–4606	5′-TAT TAG TGG TTA ATA AAT AAG G
24a	4519–4539	5′-CCC CTC TAA TAT TTA TAT ACC
25a	4675–4654	5′-TTT TAG TTA TTA GAT TAA TTA G
26a	4390–4367	5′-TAG GGA AAA AGG TTG TTA GGA TAG
Primers that amplify the sense strand		
1s	4699–4726	5′-GTA ATG ATA TTT TTT TTT TTT GTA GAG G
7s	5010–4991	5′-ATA TTA CCC TAA ATA ACC CC
9s	4603–4624	5′-GGT TTT TGT TTA TTG ATT ATT G
10s	4923–4902	5′-AAA TCT AAA TTA AAA ACC AAA C
11s	3542–3564	5′-GTG GTT TAT ATT TTT AAT TTT AG
12s	3690–3670	5′-ATT CCA AAA AAT TCA TAA TCC
13s	3673–3693	5′-TTA TGA ATT TTT TGG AAT TGG
14s	3979–3959	5′-CAC ACT ATA AAA AAA TTA CAC
15s	3461–3480	5′-GAG GAT AGT TAT AGG TTA GG
16s	3674–3655	5′-AAT CCT CTT CTA TCC TCC AC
17s	3695–3716	5′-GTT GTT GAG TTA TTT TTT TAG G
18s	3959–3938	5′-CAA AAT TCT AAA CTT TAT AAA C
19s	3958–3979	5′-TGT GTA ATT TTT TTA TAG TGT G
20s	4084–4105	5′-TTT GGA TTT GGA GTT TAG TTA G
21s	4176–4155	5′-CAA TAT TAA CTA AAA AAA TCA C
22s	4454–4476	5′-TAA AGA GTA AAT AGT TAT AGG TG
23s	4610–4590	5′-CAA AAA CCC ACC TCA CCT ATC
24s	4515–4535	5′-TTT TTT TTT TTG ATG TTT GTG
25s	4674–4653	5′-CCT AAC CAT TAA ACT AAC TAA C
26s	4391–4369	5′-ACA AAA AAA AAA ACT ACT AAA AC
Nonselective primers		
C3	4632–4650	5′-ATT TGG GGA AGA ATA AAG T
C4	4870–4852	5′-CTC AAA ACA AAC AAA CAT C
C5	4852–4870	5′-GAT GTT TGT TTG TTT TGA G
C6	5036–5018	5′-TAA CAT CCC CTC AAA ACA C

[a] Mutated bases are underlined.

for a high-density cluster of ^{m}CpGs. These replication origins include the one upstream of the β-globin gene (41) and the one designated *ors-12* (46), although only 812 bp of sequence information is available for *ors-12*.

The experimental and theoretical analyses described above suggest that a high-density cluster of ^{m}CpG dinucleotides may contribute to establishing or regulating some, if not all, replication origins in mammalian chromosomes. Such high-density ^{m}CpG clusters are missing from the *DHFR* gene in CHO cells, known to be devoid of origin activity (22, 23, 30). At the 3′ end of this gene, the density of CpGs is low (approximately one every 200 bp), though the CpGs are likely to be methylated

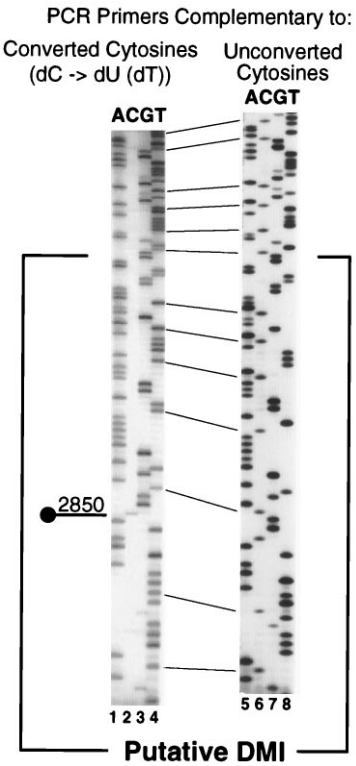

FIG. 4. Selection of genomic DNA sequences in which bisulfite had failed to convert cytosines to uracils. Total DNA was purified from proliferating CHO K1 cells and reacted with bisulfite. In lanes labeled Converted Cytosines, PCR primers 6a and 9a (Table 2) were used to amplify nucleotides 2675 to 3049 of the antisense strand DNA within ori-β. The PCR products were sequenced with primer 7a (Table 2). In lanes labeled Unconverted Cytosines, PCR primers 1D and 8D (Table 1) were used to amplify nucleotides 2675 to 3049 within ori-β. The PCR products were sequenced with primer 2E (Table 1). Thin lines identify those nucleotides that appear as cytosines in the unconverted DNA (lane 6) but as thymines in the converted DNA (lane 4). One cytosine in the converted DNA did not react with bisulfite (marked by a lollipop; lane 2).

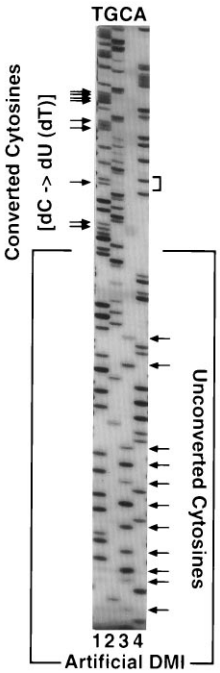

FIG. 5. An artificial DMI can be detected by the bisulfite method. An artificially constructed ori-β DMI was mixed with digested genomic DNA at molar ratios from 1/100 to 100/1. After bisulfite treatment, primers 4C (Table 1) and 21a (Table 2) were used to amplify the DMI region and primer 3E (Table 1) was used for sequencing. The 1:1 mixture is shown. Arrows indicate either unconverted cytosines or cytosines converted to thymines. The sequence spans positions 3267 (bottom) to 3379 (top). The small bracket denotes the CTA insertion between positions 3330 and 3331 created by the construction of the artificial DMI.

since the 3′ ends of the highly homologous *DHFR* genes in mice and humans are methylated (63, 65). The 5′ ends of the *DHFR* genes in mouse, human, and hamster cells contain a CpG island which is not methylated (51, 63, 65). Therefore, the *DHFR* gene lacks both origin activity and high-density clusters of mCpGs.

Dinucleotides other than CpG are not methylated at replication origins. An alternative view of DNA methylation at mammalian replication origins is that OBR are associated with a DMI in which all cytosines on both strands are methylated, regardless of their dinucleotide composition. These putative DMIs consist of well-defined loci of 516, 127, and 258 bp for ori-β, ori-RPS14 in CHO cells, and ori-RPS14 in human cells, respectively (68, 70). Moreover, they exist only in proliferating cells, not in resting cells, suggesting a role in determining where initiation of DNA replication occurs. The data supporting these conclusions were obtained by sequence analysis of genomic DNA by the bisulfite method and by digestion of genomic DNA with methylation-sensitive restriction endonucleases, followed by PCR amplification of the DMI region.

However, in our hands, neither the DMI at ori-β nor the DMI at ori-RPS14 was detected in CHO cell DNA. The bisulfite method had no difficulty detecting 35 mCpGs distributed over the 4 kb of sequence analyzed at ori-β and ori-RPS14 but failed to detect a single non-CpG methylation even though the protocol used here was capable of detecting an artificial DMI in <1% of the sample. In addition, sequence analysis of these regions by both the hydrazine and permanganate methods for identification of mC as well as with methylation-sensitive restriction endonucleases confirmed the absence of mC at non-CpG dinucleotides in the ori-β DMI locus (60). Taken together, these results make it highly unlikely that replication origins are associated with a DMI.

Others have observed continuous stretches of unconverted DNA by the bisulfite method. However, these were not interpreted as DMIs but rather as artifacts since their occurrence depended upon experimental conditions (15, 25). Likewise, we suggest that the observations reported by Tasheva and Roufa (68, 70) resulted from artifacts inherent in the two methods they used to search for DMIs. First, their restriction enzyme digestions of genomic DNA may have been incomplete, thus giving the false impression that the restriction sites analyzed were methylated. *Alu*I, for example, can easily cleave small DNA molecules but has difficulty in digesting genomic DNA to completion (60). Second, by the bisulfite method, it is critical to distinguish between DNA sequences that fail to react with bisulfite from sequences that contain mC. Bisulfite converts only cytosines in single-stranded DNA to uracils (27). Thus, stretches of unconverted DNA that characterize DMIs may have resulted from bisulfite-resistant double-stranded DNA and these stretches may have been subsequently amplified during the PCR step with primers that selectively annealed to unconverted DNA (e.g., primers P11 and P12 [68]). We have applied several different bisulfite conversion protocols (15, 25, 27, 68) to identical DNA samples and found variable percent-

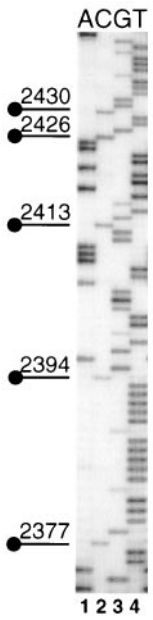

FIG. 6. Methylation pattern of newly synthesized DNA originating at ori-β. Nascent DNA was pulse-labeled at the beginning of S phase in CHO K1 cells, isolated after 6 h, and purified by affinity chromatography. DNA methylation was analyzed by the bisulfite method. Sense-strand DNA was selectively amplified with primers 2s and 3s and sequenced (lanes 1 to 4) with primer 4s. The positions of cytosines that were not converted by bisulfite are identified by lollipops.

ages of unconverted DNA with each protocol. With nonselective primers, the actual fraction of DNA that was converted could be monitored and the conditions for bisulfite treatment could be optimized. With the optimized bisulfite protocol, unconverted DNA was no longer detectable with nonselective primers but was still detectable with primers selecting for unconverted DNA, even when PCR-generated DNA without any ^{m}C was used as the starting material. Therefore, to avoid this artifact in our experiments, we chose PCR primers that selected for converted DNA sequences or PCR primers that were nonselective together with conditions that gave >95% conversion. Using our bisulfite protocol, we obtained results with DNA samples provided by Tasheva and Roufa identical to those obtained with DNA samples prepared by us from cells cultured in our own laboratory.

One would not expect this artifact to generate the well-defined transitions from regions of converted DNA to regions of unconverted DNA that defined DMIs (68). However, only one of the eight transitions that define the ori-β and ori-RPS14 DMIs was shown in a single sequencing gel lane (68). It appears that the remaining seven boundaries were assumed to exist wherever one primer set amplified unconverted DNA next to a second primer set that amplified converted DNA. However, we never observed boundaries either by sequencing the total PCR DNA product of genomic DNA (our standard procedure) or by random isolation of 15 individual clones (the standard procedure used by Tasheva and Roufa), even though we were able to sequence across the boundary of an artificial DMI (Fig. 5). We also note that the sequence data presented in documentation of one of the transitions defining the ori-RPS14 DMI (68) does not show three of the ^{m}CpGs that we found adjacent to the proposed ori-RPS14 DMI (Fig. 3 and 7) by sequencing the bulk of the amplified molecules. Thus, individual clones may not be representative of the entire DNA population.

Potential roles for methylation at replication origins. ^{m}CpGs generally are associated with transcriptionally inactive DNA (58). It is therefore surprising that some, and perhaps all, mammalian replication origins are methylated, since replication origins, like promoters, presumably require an open chromatin structure. However, the role of methylation in DNA replication may differ from that in transcription. A paradigm for methylation at replication origins is provided by the *E. coli* origin of replication. *oriC* is a 245-bp region containing 11 GATC sites that are methylated by deoxyadenosine methyltransferase (*dam*). When DNA replication is initiated at *oriC*, these sites become hemimethylated. Remethylation at *oriC* is delayed 8 min, or about 10 times longer than needed for most other locations in the *E. coli* chromosome (11, 61). The hemimethylated *oriC* is preferentially bound to the outer membrane, and this binding prevents the origin recognition protein, DnaA, from binding to *oriC* and initiating another round of replication (6, 64). Thus, the methylation status at *oriC* regulates the timing of DNA replication. Methylation at *oriC* also

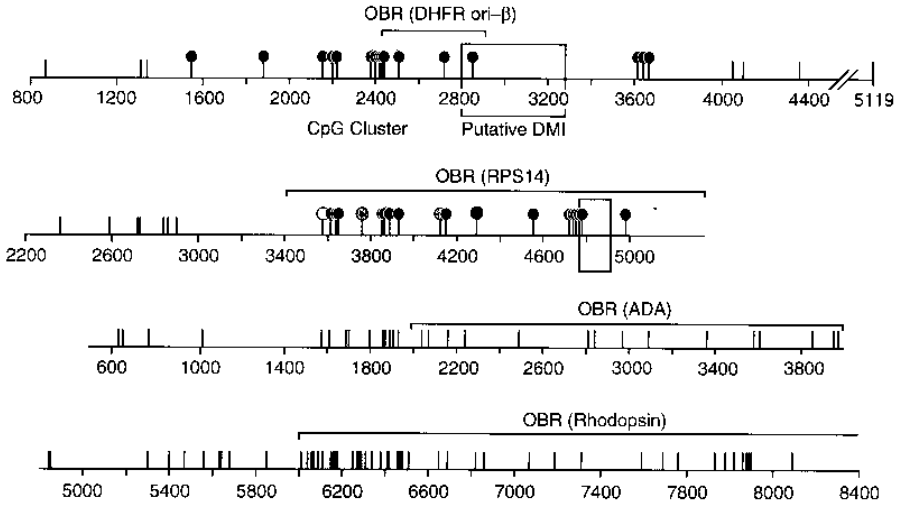

FIG. 7. Methylation patterns at different replication origins. Lollipop symbols, CpG dinucleotides analyzed in this study (filled lollipops, CpG dinucleotides methylated in all cells; shaded lollipops, CpG dinucleotides methylated in 20 to 60% of the cells); thin vertical lines, CpG dinucleotides of unknown methylation status.

influences the local DNA structure and stability (40, 77) and its interaction with replication proteins (47).

Whether methylation serves analogous functions in mammalian chromosomes remains an open question. However, certain similarities exist. For example, remethylation after replication is delayed in parts of the chromosome for up to 6 h (75). Also, mammalian cells contain proteins that preferentially bind CpG-methylated DNA in vivo, such as MeCP2 (53). In *E. coli*, the outer membrane superstructure plays a critical role in regulating replication. In mammalian chromosomes, it is clear that nuclear structure plays a role in site-specific initiation of DNA replication (30, 31, 76). Site specificity is established at mid-G_1 phase in the cell cycle (76), concurrent with the initial appearance of DNA methyltransferase activity (1, 67, 73). Hypermethylated DNA may participate in nuclear-structure-mediated establishment of origins by altering chromatin structure, either through direct DNA conformational effects of methylation (52, 79) or through specific protein-DNA interactions. Consistent with methylation-induced changes in chromatin structure are the correlations of DNA methylation with the timing of DNA replication (17, 45, 48, 62), the transcriptional activity of genes (24), and the ability of DNA to undergo homologous recombination (36). Experiments are in progress to test some of these hypotheses.

ACKNOWLEDGMENTS

M.L.D. and H.Z. were coprincipal investigators.

T.R. was supported by a postdoctoral fellowship from the Deutsche Forschungsgemeinschaft. This work was supported in part by grant Zo 59/2-2 from the Deutsche Forschungsgemeinschaft awarded to H.Z.

We thank E.-L. Winnacker for his continuing support, D. A. Natale for insightful comments on the manuscript, and Elena Tasheva and Donald Roufa for a free and open exchange of results and ideas and for providing samples of their DNA.

REFERENCES

1. **Adams, R. L. P.** 1990. DNA methylation. Biochem. J. **265:**309–320.
2. **Aladjem, M. I., M. Groudine, L. L. Brody, E. S. Dieken, R. E. Fournier, G. M. Wahl, and E. M. Epner.** 1995. Participation of the human β-globin locus control region in initiation of DNA replication. Science **270:**815–819.
3. **Anachkova, B., and J. Hamlin.** 1989. Replication in the amplified dihydrofolate reductase domain in CHO cells may initiate at two distinct sites, one of which is a repetitive sequence element. Mol. Cell. Biol. **9:**532–540.
4. **Berberich, S., A. Trivedi, D. C. Daniel, E. M. Johnson, and M. Leffak.** 1995. In vitro replication of plasmids containing human c-myc DNA. J. Mol. Biol. **245:**92–109.
5. **Blow, J. J., and A. M. Sleeman.** 1990. Replication of purified DNA in *Xenopus* egg extract is dependent on nuclear assembly. J. Cell Sci. **95:**383–391.
6. **Brendler, T., A. Abeles, and S. Austin.** 1995. A protein that binds to the P1 origin core and the *oriC* 13mer region in a methylation-specific fashion is the product of the host *seqA* gene. EMBO J. **14:**4083–4089.
7. **Burhans, W. C., J. E. Selegue, and N. H. Heintz.** 1986. Isolation of the origin of replication associated with the amplified Chinese hamster dihydrofolate reductase domain. Proc. Natl. Acad. Sci. USA **83:**7790–7794.
8. **Burhans, W. C., J. E. Selegue, and N. H. Heintz.** 1986. Replication intermediates formed during initiation of DNA synthesis in methotrexate-resistant CHO C400 cells enriched for sequences derived from a specific, amplified restriction fragment. Biochemistry **25:**441–449.
9. **Burhans, W. C., L. T. Vassilev, M. S. Caddle, N. H. Heintz, and M. L. DePamphilis.** 1990. Identification of an origin of bidirectional replication. Cell **62:**955–965.
10. **Burhans, W. C., L. T. Vassilev, J. Wu, J. M. Sogo, F. S. Nallaseth, and M. L. DePamphilis.** 1991. Emetine allows identification of origins of mammalian DNA replication by imbalanced DNA synthesis, not through conservative nucleosome segregation. EMBO J. **10:**4351–4360.
11. **Campbell, J. L., and N. Kleckner.** 1990. E. coli *oriC* and the *dnaA* gene promoter are sequestered from dam methyltransferase following the passage of the chromosomal replication fork. Cell **62:**967–979.
12. **Carroll, S. M., M. L. DeRose, J. L. Kolman, G. H. Nonet, R. E. Kelly, and G. M. Wahl.** 1993. Localization of a bidirectional DNA replication origin in the native locus and in episomally amplified murine adenosine deaminase loci. Mol. Cell. Biol. **13:**2971–2981.
13. **Cedar, H.** 1988. DNA methylation and gene activity. Cell **53:**3–4.
14. **Cheng, X.** 1995. Structure and function of DNA methyltransferase. Annu. Rev. Biophys. Biomol. Struct. **24:**293–318.
15. **Clark, S. J., J. Harrison, C. L. Paul, and M. Frommer.** 1994. High sensitivity mapping of methylated cytosines. Nucleic Acids Res. **22:**2990–2997.

15a. **Cooney, C. A., R. L. Eykholt, and E. M. Bradbury.** 1988. Methylation is coordinated on the putative replication origins of *Physarum* ribosomal DNA. J. Mol. Biol. **204:**889–901.

16. **Cox, L.** 1992. DNA replication in cell-free extract from Xenopus is prevented by disrupting nuclear envelope function. J. Cell Sci. **101:**43–53.
17. **Craig, J. M., and W. A. Bickmore.** 1994. The distribution of CpG islands in mammalian chromosomes. Nat. Genet. **7:**376–382.
18. **DePamphilis, M. L.** 1993. Eukaryotic DNA replication: anatomy of an origin. Annu. Rev. Biochem. **62:**29–63.
19. **DePamphilis, M. L.** 1993. Origins of DNA replication in metazoan chromosomes. J. Biol. Chem. **268:**1–4.
20. **DePamphilis, M. L.** 1993. Origins of DNA replication that function in eukaryotic cells. Curr. Opin. Cell Biol. **5:**434–441.
21. **DePamphilis, M. L.** 1996. DNA replication origins, p. 45–86. *In* M. L. DePamphilis (ed.), DNA replication in eukaryotic cells. Cold Spring Harbor Laboratory, Cold Spring Harbor, N.Y.
22. **Dijkwel, P. A., and J. L. Hamlin.** 1995. The Chinese hamster dihydrofolate reductase origin consists of multiple potential nascent-strand start sites. Mol. Cell. Biol. **15:**3023–3031.
23. **Dijkwel, P. A., J. P. Vaughn, and J. L. Hamlin.** 1994. Replication initiation sites are distributed widely in the amplified CHO dihydrofolate reductase domain. Nucleic Acids Res. **22:**4989–4996.
24. **Eden, S., and H. Cedar.** 1994. Role of DNA methylation in the regulation of transcription. Curr. Opin. Genet. Dev. **4:**255–259.
25. **Feil, R., J. Charlton, A. P. Bird, J. Walter, and W. Reik.** 1994. Methylation analysis on individual chromosomes: improved protocol for bisulphite genomic sequencing. Nucleic Acids Res. **22:**695–696.
26. **Ferguson, A. T., R. G. Lapidus, S. B. Baylin, and N. E. Davidson.** 1995. Demethylation of the estrogen receptor gene in estrogen receptor-negative breast cancer cells can reactivate estrogen receptor gene expression. Cancer Res. **55:**2279–2283.
27. **Frommer, M., L. E. McDonald, D. S. Millar, C. M. Collis, F. Watt, G. W. Grigg, P. L. Molloy, and C. L. Paul.** 1992. A genomic sequencing protocol that yields a positive display of 5-methylcytosine residues in individual DNA strands. Proc. Natl. Acad. Sci. USA **89:**1827–1831.
28. **Gale, J. M., R. A. Tobey, and J. A. D'Anna.** 1992. Localization and DNA sequence of a replication origin in the rhodopsin gene locus of Chinese hamster cells. J. Mol. Biol. **224:**343–358.
29. **Giacca, M., L. Zentilin, P. Norio, S. Diviacco, D. Dimitrova, G. Contreas, G. Biamonti, G. Perini, F. Weighardt, S. Riva, and A. Falaschi.** 1994. Fine mapping of a replication origin of human DNA. Proc. Natl. Acad. Sci. USA **91:**7119–7123.
30. **Gilbert, D. M., H. Miyazawa, and M. L. DePamphilis.** 1995. Site-specific initiation of mammalian DNA replication in *Xenopus* egg extracts requires nuclear structure. Mol. Cell. Biol. **15:**2942–2954.
31. **Gilbert, D. M., H. Miyazawa, F. S. Nallaseth, J. M. Ortega, J. J. Blow, and M. L. DePamphilis.** 1994. Site-specific initiation of DNA replication in metazoan chromosomes and the role of nuclear organization. Cold Spring Harbor Symp. Quant. Biol. **58:**475–485.
32. **Gogel, E., G. Langst, I. Grummt, E. Kunkel, and F. Grummt.** 1996. Mapping of origin initiation sites in the mouse ribosomal gene cluster. Chromosoma **104:**511–518.
33. **Handeli, S., A. Klar, M. Meuth, and H. Cedar.** 1989. Mapping replication units in animal cells. Cell **57:**909–920.
34. **Heintz, N. H., and J. L. Hamlin.** 1982. An amplified chromosomal sequence that includes the gene for dihydrofolate reductase initiates replication within specific restriction fragments. Proc. Natl. Acad. Sci. USA **79:**4083–4087.
35. **Heintz, N. H., and B. W. Stillman.** 1988. Nuclear DNA synthesis in vitro is mediated via stable replication forks assembled in a temporally specific fashion in vivo. Mol. Cell. Biol. **8:**1923–1931.
36. **Hsieh, C.-L., and M. R. Lieber.** 1992. CpG methylated minichromosomes become inaccessible for V(D)J recombination after undergoing replication. EMBO J. **11:**315–325.
37. **Hyrien, O., C. Maric, and M. Méchali.** 1995. Transition in specification of embryonic metazoan DNA replication origins. Science **270:**994–997.
38. **Jenkins, H., T. Holman, C. Lyon, B. Lane, R. Stick, and C. Hutchison.** 1993. Nuclei that lack a lamina accumulate karyophilic proteins and assemble a nuclear matrix. J. Cell Sci. **106:**275–285.
39. **Kelly, R. E., M. L. DeRose, B. W. Draper, and G. M. Wahl.** 1995. Identification of an origin of bidirectional DNA replication in the ubiquitously expressed mammalian *CAD* gene. Mol. Cell. Biol. **15:**4136–4148.
40. **Kimura, T., T. Asai, M. Imai, and M. Takanami.** 1989. Methylation strongly enhances DNA bending in the replication origin region of the *Escherichia coli* chromosome. Mol. Gen. Genet. **219:**69–74.
41. **Kitsberg, D., S. Selig, I. Keshet, and H. Cedar.** 1993. Replication structure of the human β-globin gene domain. Nature **366:**588–590.
42. **Kobayashi, T., and M. L. DePamphilis.** Unpublished results.
43. **Krysan, P. J., J. G. Smith, and M. P. Calos.** 1993. Autonomous replication

in human cells of multimers of specific human and bacterial sequences. Mol. Cell. Biol. **13:**2688–2696.
44. **Leu, T.-H., and J. L. Hamlin.** 1989. High-resolution mapping of replication fork movement through the amplified dihydrofolate reductase domain in CHO cells by in-gel renaturation analysis. Mol. Cell. Biol. **9:**523–531.
45. **Lin, M. S., A. Zhang, and A. Fujimoto.** 1995. Asynchronous DNA replication between 15q11.2q12 homologs: cytogenetic evidence for maternal imprinting and delayed replication. Hum. Genet. **96:**572–576.
46. **Mah, D. C., P. A. Dijkwel, A. Todd, V. Klein, G. B. Price, and M. Zannis-Hadjopoulos.** 1993. ors12, a mammalian autonomously replicating DNA sequence, associates with the nuclear matrix in a cell cycle-dependent manner. J. Cell Sci. **105:**807–818.
47. **Marians, K. J.** 1992. Prokaryotic DNA replication. Annu. Rev. Biochem. **61:**673–719.
48. **McQueen, H. A., J. Fantes, S. H. Cross, V. H. Clark, A. L. Archibald, and A. P. Bird.** 1996. CpG islands of chicken are concentrated on minichromosomes. Nat. Genet. **12:**321–324.
49. **McWinney, C., S. E. Waltz, and M. Leffak.** 1995. Cis-acting effects of sequences within 2.4-kb upstream of the human c-myc gene on autonomous plasmid replication in HeLa cells. DNA Cell Biol. **14:**565–579.
50. **Meehan, R. R., J. D. Lewis, and A. P. Bird.** 1992. Characterization of MeCP2, a vertebrate DNA binding protein with affinity for methylated DNA. Nucleic Acids Res. **20:**5085–5092.
51. **Mitchell, P. J., A. M. Carothers, J. H. Han, J. D. Harding, E. Kas, L. Venolia, and L. A. Chasin.** 1986. Multiple transcription start sites, DNase I-hypersensitive sites, and an opposite-strand exon in the 5′ region of the CHO *dhfr* gene. Mol. Cell. Biol. **6:**425–440.
52. **Murchie, A. I. H., and D. M. J. Lilley.** 1989. Base methylation and local DNA helix stability: effect on the kinetics of cruciform extrusion. J. Mol. Biol. **205:**593–602.
53. **Nan, X., P. Tate, E. Li, and A. Bird.** 1996. DNA methylation specifies chromosomal localization of MeCP2. Mol. Cell. Biol. **16:**414–421.
54. **Newport, J. W., K. L. Wilson, and W. G. Dunphy.** 1990. A lamin-independent pathway for nuclear envelope assembly. J. Cell Biol. **111:**2247–2259.
55. **Öfverstedt, L. G., K. Hammarström, N. Balgobin, S. Hjerten, U. Pettersson, and J. Chattopadhaya.** 1984. Rapid and quantitative recovery of DNA fragments from gels by displacement electrophoresis (isotachophoresis). Biochim. Biophys. Acta **782:**120–126.
56. **Orr-Weaver, T. L.** 1991. Drosophila chorion genes: cracking the eggshell's secrets. Bioessays **13:**97–105.
57. **Pelizon, C., S. Diviacco, A. Falaschi, and M. Giacca.** 1996. High-resolution mapping of the origin of DNA replication in the hamster dihydrofolate reductase gene domain by competitive PCR. Mol. Cell. Biol. **16:**5358–5364.
58. **Razin, A., and T. Kafri.** 1994. DNA methylation from embryo to adult. Prog. Nucleic Acid Res. Mol. Biol. **48:**53–81.
59. **Reilly, J. G., C. A. Thomas, and M. J. Lundell.** 1982. Methylation of mouse ribosomal RNA genes. DNA **1:**259–266.
60. **Rein, T., D. Natale, U. Gärtner, M. Niggemann, M. L. DePamphilis, and H. Zorbas.** Absence of an unusual "densely methylated island" at the hamster DHFR ori-β. Submitted for publication.
61. **Russell, D. W., and N. D. Zinder.** 1987. Hemimethylation prevents DNA replication in E. coli. Cell **50:**1071–1079.
62. **Selig, S., M. Ariel, R. Goitein, M. Marcus, and H. Cedar.** 1988. Regulation of mouse satellite DNA replication time. EMBO J. **7:**419–426.
63. **Shimada, T., and A. W. Nienhuis.** 1985. Only the promoter region of the constitutively expressed normal and amplified human dihydrofolate reductase gene is DNase I hypersensitive and undermethylated. J. Biol. Chem. **260:**2468–2474.
64. **Slater, S., S. Wold, M. Lu, E. Boye, K. Skarstad, and N. Kleckner.** 1995. E. coli SeqA protein binds *oriC* in two different methyl-modulated reactions appropriate to its roles in DNA replication initiation and origin sequestration. Cell **82:**927–936.
65. **Stein, R., N. Sciaky-Gallili, A. Razin, and H. Cedar.** 1983. Pattern of methylation of two genes coding for housekeeping functions. Proc. Natl. Acad. Sci. USA **80:**2422–2426.
66. **Swisshelm, K., C. M. Disteche, J. Thorvaldsen, A. Nelson, and D. Salk.** 1990. Age-related increase in methylation of ribosomal genes and inactivation of chromosome-specific rRNA gene clusters in mouse. Mutat. Res. **237:**131–146.
67. **Szyf, M., V. Bozovic, and G. Tanigawa.** 1991. Growth regulation of mouse DNA methyltransferase gene expression. J. Biol. Chem. **266:**10027–10030.
68. **Tasheva, E. S., and D. J. Roufa.** 1994. Densely methylated DNA islands in mammalian chromosomal replication origins. Mol. Cell. Biol. **14:**5636–5644.
69. **Tasheva, E. S., and D. J. Roufa.** 1994. A mammalian origin of bidirectional DNA replication within the Chinese hamster *RPS14* locus. Mol. Cell. Biol. **14:**5628–5635.
70. **Tasheva, E. S., and D. J. Roufa.** 1995. A densely methylated DNA island is associated with a chromosomal replication origin in the human RPS14 locus. Somatic Cell Mol. Genet. **19:**369–383.
71. **Vassilev, L. T., W. C. Burhans, and M. L. DePamphilis.** 1990. Mapping an origin of bidirectional replication at a single-copy locus in exponentially proliferating mammalian cells. Mol. Cell. Biol. **10:**4685–4689.
72. **Virta-Pearlman, V. J., P. H. Gunaratne, and A. C. Chinault.** 1993. Analysis of a replication initiation sequence from the adenosine deaminase region of the mouse genome. Mol. Cell. Biol. **13:**5931–5942.
73. **Vogel, M. C., T. Papadopoulos, H. K. Müller-Hermelink, D. Drahovsky, and G. P. Pfeifer.** 1988. Intracellular distribution of DNA methyltransferase during the cell cycle. FEBS Lett. **236:**9–13.
74. **Woodcock, D. M., P. J. Crowther, and W. P. Diver.** 1987. The majority of methylated deoxycytidines in human DNA are not in the CpG dinucleotide. Biochem. Biophys. Res. Commun. **145:**888–894.
75. **Woodcock, D. M., D. L. Simmons, P. J. Crowther, I. A. Cooper, K. J. Trainor, and A. A. Morley.** 1986. Delayed DNA methylation is an integral feature of DNA replication in mammalian cells. Exp. Cell Res. **166:**102–112.
76. **Wu, S., and D. Gilbert.** 1996. A distinct G1-phase step required to specify a mammalian replication origin. Science **271:**1270–1272.
77. **Yamaki, H., E. Ohtsubo, K. Nagai, and Y. Maeda.** 1988. The oriC unwinding by dam methylation in Escherichia coli. Nucleic Acids Res. **16:**5067–5073.
78. **Yoon, Y., J. A. Sanchez, C. Brun, and J. A. Huberman.** 1995. Mapping of replication initiation sites in human ribosomal DNA by nascent-strand abundance analysis. Mol. Cell. Biol. **15:**2482–2489.
79. **Zacharias, W., T. R. O'Connor, and J. E. Larson.** 1988. Methylation of cytosine in the 5-position alters the structural and energetic properties of the supercoiled-induced Z-helix and of B-Z junctions. Biochemistry **27:**2970–2978.